A Differential-Algebraic Approach to Speed Estimation in an Induction Motor: Open Loop Experimental Results

Mengwei Li, John Chiasson, Marc Bodson, and Leon M. Tolbert

***Abstract*— Previous work by the authors has described a differential-algebraic approach to speed estimation in induction motors. The method shows that the speed ω can be found by solving for the roots of a polynomial in ω whose coefficients are functions of the stator voltages, stator currents, and their derivatives. Preliminary experimental results are presented in which the speed is estimated using the differential-algebraic method.**

***Index Terms*— Sensorless Speed Observer, Induction Motor**

I. Introduction

Sensorless control of an induction motor refers to the problem of controlling it without the use of a rotor position/speed sensor. Many different techniques have been proposed to estimate the speed of an induction motor without a speed sensor. This area has a rather large literature, and the reader is referred to [1][2][3][4][5][6][7][8] for an exposition of many of the existing approaches. The approach presented in this work is most closely related to the ideas described in [9][10][11][12][13]. In [9][10][11][12], observability is characterized as being able to reconstruct the unknown state variables as rational functions of the inputs, outputs, and their derivatives (See [10][11][12] for a more precise definition). The authors have shown in [14] that the speed ω can be found by solving for the roots of a polynomial in ω whose coefficients are functions of the stator voltages, stator currents, and their derivatives. Simulations have shown that this speed estimate can be used in a field-oriented controller to obtain tracking control of the machine for low-speed (including zero speed) trajectories under full load. However, it does require a small time step size (1 μsec) to be able to reconstruct the derivatives of the stator voltages and the stator currents. The control of the machine in real time requires a sample period of 120 μsec with the computing platform used by the authors. As a consequence, we consider only the reconstruction of the speed from the stator voltages and stator currents. This is an open-loop procedure in that the estimated speed is not fed back for real-time control of the machine. More specifically, the work here describes preliminary experimental results in which the speed is estimated using the algorithm given in Li et al [14], but the estimate is not used for feedback control. The rest of the paper is structured as follows. Section II describes the mathematical model of an induction motor, Section III presents the differential-algebraic speed observer, Section IV presents the stabilized speed observer, Section V gives some simulation results, and Section VI gives the experimental results. The last section gives some conclusions and future considerations.

M. Li and J. Chiasson are with the ECE Department, The University of Tennessee, Knoxville, TN 37996, mwl@utk.edu, chiasson@utk.edu

M. Bodson is with the ECE Department, The University of Utah, Salt Lake City, UT 84112, bodson@ee.utah.edu.

L. M. Tolbert is with the ECE Department, The University of Tennessee, Knoxville, TN 37996, tolbert@utk.edu and The Oak Ridge National Laboratory, Oak Ridge TN, tolbertlm@ornl.gov.

Drs. Chiasson and Tolbert would like to thank Oak Ridge National Laboratory for partially supporting this work through the UT/Battelle contract no. 4000007596. Dr. Tolbert would also like to thank the National Science Foundation for partially supporting this work through contract NSF ECS-0093884.

II. Mathematical Model of the Induction Motor

With $\underline{i}_S \triangleq i_{Sa} + ji_{Sb}$, $\underline{\psi}_R \triangleq \psi_{Ra} + j\psi_{Rb}$, and $\underline{u}_S \triangleq u_{Sa} + ju_{Sb}$, a two-phase equivalent state-space mathematical model of the induction motor in space vector form is given by (see [15])

$$\frac{d}{dt}\underline{i}_S = \frac{\beta}{T_R}\left(1 - jn_P\omega T_R\right)\underline{\psi}_R - \gamma\underline{i}_S + \frac{1}{\sigma L_S}\underline{u}_S \quad (1)$$

$$\frac{d}{dt}\underline{\psi}_R = -\frac{1}{T_R}\left(1 - jn_P\omega T_R\right)\underline{\psi}_R + \frac{M}{T_R}\underline{i}_S \quad (2)$$

$$\frac{d\omega}{dt} = \frac{n_p M}{J L_R}\operatorname{Im}\left\{\underline{i}_S\underline{\psi}_R^*\right\} - \frac{\tau_L}{J} \quad (3)$$

where, θ is the position of the rotor, $\omega = d\theta/dt$, n_p is the number of pole pairs, i_{Sa}, i_{Sb} are the (two phase equivalent) stator currents, u_{Sa}, u_{Sb} are the (two phase equivalent) stator voltages, and ψ_{Ra}, ψ_{Rb} are the (two phase equivalent) rotor flux linkages, R_S and R_R are the stator and rotor resistances, M is the mutual inductance, L_S and L_R are the stator and rotor inductances, J is the inertia of the rotor, and τ_L is the load torque. The symbols

$$T_R = \frac{L_R}{R_R} \qquad \sigma = 1 - \frac{M^2}{L_S L_R}$$

$$\beta = \frac{M}{\sigma L_S L_R} \qquad \gamma = \frac{R_S}{\sigma L_S} + \frac{1}{\sigma L_S}\frac{1}{T_R}\frac{M^2}{L_R}$$

have been used to simplify the expressions. T_R is referred to as the rotor time constant, and σ is called the total leakage factor.

III. Differential-Algebraic Speed Observer

Differentiating (1) gives

$$\frac{d^2}{dt^2}\underline{i}_S = \frac{\beta}{T_R}\left(1 - jn_P\omega T_R\right)\frac{d}{dt}\underline{\psi}_R - jn_P\beta\underline{\psi}_R\frac{d\omega}{dt} - \gamma\frac{d}{dt}\underline{i}_S + \frac{1}{\sigma L_S}\frac{d}{dt}\underline{u}_S. \quad (4)$$

Using the complex-valued equations (1) and (2), one can eliminate $\underline{\psi}_R$ and $\frac{d}{dt}\underline{\psi}_R$ from (4) to obtain

$$\begin{aligned}\frac{d^2}{dt^2}\underline{i}_S =& -\frac{1}{T_R}\left(1 - jn_P\omega T_R\right)\left(\frac{d}{dt}\underline{i}_S + \gamma\underline{i}_S - \frac{1}{\sigma L_S}\underline{u}_S\right)\\ &+ \frac{\beta M}{T_R^2}\left(1 - jn_P\omega T_R\right)\underline{i}_S - \gamma\frac{d}{dt}\underline{i}_S + \frac{1}{\sigma L_S}\frac{d}{dt}\underline{u}_S\\ &- \frac{jn_P T_R}{1 - jn_P\omega T_R}\left(\frac{d}{dt}\underline{i}_S + \gamma\underline{i}_S - \frac{1}{\sigma L_S}\underline{u}_S\right)\frac{d\omega}{dt}.\end{aligned} \quad (5)$$

Solving (5) for $d\omega/dt$ gives

$$\frac{d\omega}{dt} = -\frac{\left(1 - jn_P\omega T_R\right)^2}{jn_P T_R^2} + \frac{1 - jn_P\omega T_R}{jn_P T_R}\times \frac{\frac{\beta M}{T_R^2}\left(1 - jn_P\omega T_R\right)\underline{i}_S - \gamma\frac{d}{dt}\underline{i}_S + \frac{1}{\sigma L_S}\frac{d}{dt}\underline{u}_S - \frac{d^2}{dt^2}\underline{i}_S}{\frac{d}{dt}\underline{i}_S + \gamma\underline{i}_S - \frac{1}{\sigma L_S}\underline{u}_S}. \quad (6)$$

If the signals are measured exactly and the dynamic model is correct, the right-hand side must be real. From (1) it is seen that the denominator in the last term of (6) is equal to $\left(\beta/T_R\right)\left(1 - jn_P\omega T_R\right)\underline{\psi}_R$ and thus (6) is singular (i.e., the denominator in (6) is zero), if and only if $\left|\underline{\psi}_R\right| \equiv 0$.

Breaking down the right-hand side of (6) into its real and imaginary parts, the real part has the form

$$\begin{aligned}\frac{d\omega}{dt} =\ & a_2\left(u_{Sa}, u_{Sb}, i_{Sa}, i_{Sb}\right)\omega^2 + a_1\left(u_{Sa}, u_{Sb}, i_{Sa}, i_{Sb}\right)\omega\\ &+ a_0\left(u_{Sa}, u_{Sb}, i_{Sa}, i_{Sb}\right).\end{aligned} \quad (7)$$

The expressions for $a_2\left(u_{Sa}, u_{Sb}, i_{Sa}, i_{Sb}\right)$, $a_1\left(u_{Sa}, u_{Sb}, i_{Sa}, i_{Sb}\right)$, and $a_0\left(u_{Sa}, u_{Sb}, i_{Sa}, i_{Sb}\right)$ are lengthy and therefore not explicitly presented here (Appendix VIII-B gives their steady-state expressions). It is shown in [14] that (7) is never stable in steady state and thus cannot be used as an observer by just integrating it in real time.

On the other hand, the imaginary part of (6) has no derivatives in the speed leading to a second-degree polynomial equation in ω of the form

$$\begin{aligned}q(\omega) \triangleq\ & q_2(u_{Sa}, u_{Sb}, i_{Sa}, i_{Sb})\omega^2 + q_1(u_{Sa}, u_{Sb}, i_{Sa}, i_{Sb})\omega\\ &+ q_0(u_{Sa}, u_{Sb}, i_{Sa}, i_{Sb}).\end{aligned} \quad (8)$$

If ω is the speed of the motor, then $q(\omega)$ is zero. The expressions for $q_2(u_{Sa}, u_{Sb}, i_{Sa}, i_{Sb})$, $q_1\left(u_{Sa}, u_{Sb}, i_{Sa}, i_{Sb}\right)$, and $q_0(u_{Sa}, u_{Sb}, i_{Sa}, i_{Sb})$ are lengthy and not explicitly presented here (Their steady-state expressions are given in Appendix VIII-A.). There are two solutions to (8), and at least one of these two solutions must track the motor speed. This equation does not have a stability issue, but a procedure is required to determine which of the two solutions is correct. Further, there are situations where the speed cannot be determined by (8). For example, if u_{Sa} = constant and $u_{Sb} = 0$, it turns out that $q_2(u_{Sa}, u_{Sb}, i_{Sa}, i_{Sb}) = q_1(u_{Sa}, u_{Sb}, i_{Sa}, i_{Sb}) = q_0(u_{Sa}, u_{Sb}, i_{Sa}, i_{Sb}) \equiv 0$ and ω is not determinable from (8)[1]. On the other hand, if the machine is operated at zero speed ($\omega \equiv 0$) with a load on it, then $q_2(u_{Sa}, u_{Sb}, i_{Sa}, i_{Sb}) \equiv 0$ and $q_1(u_{Sa}, u_{Sb}, i_{Sa}, i_{Sb}) \neq 0$, and a unique solution is specified by (8) (see Appendix VIII-A where this is proved in steady state). In fact, for low speed trajectories, consider equation (8) written in the form

$$\left(q_2\omega + q_1\right)\omega + q_0 = 0. \quad (9)$$

At low speeds, defined by $\left|q_2\omega\right| \ll \left|q_1\right|$, (9) reduces to

$$q_1\omega + q_0 = 0$$

and ω is uniquely determined by $\omega = -q_0/q_1$. (It is shown in [14] that in steady state, $\left|q_2\omega\right| \ll \left|q_1\right|$ if $\left(T_R n_p\omega\right)^2 \ll 1$.)

If $q_2(u_{Sa}, u_{Sb}, i_{Sa}, i_{Sb}) \neq 0$, one determines the correct solution of (8) as follows: Differentiate equation (8) to obtain the new independent equation

$$\left(2q_2\omega + q_1\right)\frac{d\omega}{dt} + \dot{q}_2\omega^2 + \dot{q}_1\omega + \dot{q}_0 \equiv 0. \quad (10)$$

Next, $d\omega/dt$ is replaced by the right-hand side of equation (7) to obtain a new algebraic polynomial equation in ω given by

$$\begin{aligned}g(\omega) \triangleq\ & 2q_2a_2\omega^3 + \left(2q_2a_1 + q_1a_2 + \dot{q}_2\right)\omega^2\\ &+ \left(2q_2a_0 + q_1a_1 + \dot{q}_1\right)\omega + q_1a_0 + \dot{q}_0.\end{aligned} \quad (11)$$

$g(\omega)$ is a third-order polynomial equation in ω for which the speed of the motor is one of its roots. Dividing[2] (11) by $q(\omega)$ from (8), the polynomial (11) has the form

$$\begin{aligned}g(\omega) =\ & \left(2q_2a_2\omega + 2q_2a_1 - q_2q_1a_2 + \dot{q}_2\right)q(\omega)\\ &+ r_1\left(u_{Sa}, u_{Sb}, i_{Sa}, i_{Sb}\right)\omega + r_0\left(u_{Sa}, u_{Sb}, i_{Sa}, i_{Sb}\right).\end{aligned} \quad (12)$$

where

$$\begin{aligned}r_1\left(u_{Sa}, u_{Sb}, i_{Sa}, i_{Sb}\right) \triangleq\ & 2q_2^2a_0 - q_2q_1a_1 + q_2\dot{q}_1\\ &- 2q_2q_0a_2 + q_1^2a_2 - q_1\dot{q}_2\end{aligned} \quad (13)$$

and

$$\begin{aligned}r_0\left(u_{Sa}, u_{Sb}, i_{Sa}, i_{Sb}\right) \triangleq\ & q_2q_1a_0 + q_2\dot{q}_0 - 2q_2q_0a_1\\ &+ q_0q_1a_2 - q_0\dot{q}_2.\end{aligned} \quad (14)$$

If ω is equal to the speed of the motor, then both $g(\omega) = 0$ and $q(\omega) = 0$, and one obtains

$$r(\omega) \triangleq r_1\left(u_{Sa}, u_{Sb}, i_{Sa}, i_{Sb}\right)\omega + r_0\left(u_{Sa}, u_{Sb}, i_{Sa}, i_{Sb}\right) = 0. \quad (15)$$

This is now a first-order polynomial equation in ω with a unique solution as long as r_1 (the coefficient of ω) is

[1] An induction machine is not typically operated under these conditions. See [13] for more discussion of this issue.

[2] Given the polynomials $g(\omega), q(\omega)$ in ω with $\deg\{g(\omega)\} = n_g, \deg\{q(\omega)\} = n_q$, the Euclidean division algorithm ensures that there are polynomials $\gamma(\omega), r(\omega)$ such that $g(\omega) = \gamma(\omega)q(\omega) + r(\omega)$ and $\deg\{r(\omega)\} \leq \deg\{q(\omega)\} - 1 = n_q - 1$. Consequently, if ω_0 is a zero of both $g(\omega)$ and $q(\omega)$, then it must also be a zero of $r(\omega)$.

nonzero (It is shown in [14] that $r_1 \neq 0$ in steady state if $q_2 \neq 0$). The coefficients of r_1, r_0 contain 3^{rd} derivatives of the stator currents and 2^{nd} derivatives of the stator voltages and, therefore, noise is a concern. Rather than use this purely algebraic estimator, it is now shown how to combine it with the dynamic model to obtain a smoother (yet stable) speed estimator.

IV. Stable Dynamic Speed Observer

Dividing the right side of the differential equation model (7) by $q(\omega)$ $(q_2(u_{Sa}, u_{Sb}, i_{Sa}, i_{Sb}) \neq 0)$, one obtains

$$a_2\omega^2 + a_1\omega + a_0 = \gamma \times q(\omega) + \alpha\omega + \beta \tag{16}$$

where

$$\alpha \triangleq a_1 - a_2 q_1/q_2 \tag{17}$$

and

$$\beta \triangleq a_0 - a_2 q_0/q_2. \tag{18}$$

Then, as $q(\omega) \equiv 0$, (7) may be rewritten as

$$\frac{d\omega}{dt} = \alpha(t)\omega + \beta(t) \tag{19}$$

which is a *linear first-order time-varying* system. With

$$\Phi(t, t_0) \triangleq e^{\int_{t_0}^{t} \alpha(\tau)d\tau}$$

the fundamental solution of (19), the full solution is given by (see [16])

$$\omega(t) = \Phi(t, t_0)\omega(0) + \int_{t_0}^{t} \Phi(t, \tau)\beta(\tau)d\tau.$$

Consequently, a sufficient condition for stability is that $\alpha(t) \leq -\kappa < 0$ for some $\kappa > 0$. It is shown in Appendix VIII-B that $\alpha > 0$ in steady state, so the system is never stable in steady state.

For the case that $q_2\,(u_{Sa}, u_{Sb}, i_{Sa}, i_{Sb}) \neq 0$, consider (19) to be the induction motor "model" and the solution ω of algebraic estimator (15) to be the "measurement". Then, let an observer be defined by

$$\frac{d\hat{\omega}}{dt} = \alpha(t)\hat{\omega} + \beta(t) + \ell\,(\omega - \hat{\omega})\,. \tag{20}$$

If $\ell - \alpha(t) > \kappa > 0$ for all t, then the estimator (20) is stable with a rate of decay of the error no less than κ. As this estimator is the result of integrating the signals $\alpha(t)$, $\beta(t)$, and ω (from (15)), it is a smoother estimate than the purely algebraic estimate.

In the case where $q_2\,(u_{Sa}, u_{Sb}, i_{Sa}, i_{Sb}) = 0$, then the right side of equation (7) can be divided by $q_1\,(u_{Sa}, u_{Sb}, i_{Sa}, i_{Sb})\,\omega + q_0\,(u_{Sa}, u_{Sb}, i_{Sa}, i_{Sb}) = 0$ to obtain

$$\frac{d\hat{\omega}}{dt} = c(t) + \ell\,(\omega - \hat{\omega})\,. \tag{21}$$

If $\ell > \kappa > 0$ for all t, then (21) is stable with a rate of decay of the error no less than κ.

The estimate of speed proposed here is defined as the solution to the observer

$$\begin{aligned}\frac{d\hat{\omega}}{dt} \triangleq\ & a_2\,(u_{Sa}, u_{Sb}, i_{Sa}, i_{Sb})\,\hat{\omega}^2 + a_1\,(u_{Sa}, u_{Sb}, i_{Sa}, i_{Sb})\,\hat{\omega} \\ & + a_0\,(u_{Sa}, u_{Sb}, i_{Sa}, i_{Sb}) + \ell\,(\omega - \hat{\omega})\end{aligned} \tag{22}$$

where

$$\omega \triangleq \begin{cases} -q_0/q_1 & \text{if } |q_2\hat{\omega}| \leq 0.05\,|q_1| \quad \text{[See (8)]} \\ -r_0/r_1 & \text{if } |q_2\hat{\omega}| > 0.05\,|q_1| \quad \text{[See (15)].} \end{cases}$$

In Appendix VIII-A it is shown that in steady state $q_1 \neq 0$ if $q_2 = 0$, while in Appendix **??** it is shown that $r_1 \neq 0$ if $q_2 \neq 0$.

V. Simulation Results

As a first look at the viability of the observer (22), simulations were conducted to test it. Here, a three-phase (two-phase equivalent) induction motor model was simulated using SIMULINK with parameter values chosen to be

$$\begin{aligned} n_p = 2,\ R_S = 5.12 \text{ ohms},\ R_R = 2.23 \text{ ohms}, \\ L_S = L_R = 0.2919 \text{ H},\ M = 0.2768 \text{ H}, \\ J = 0.0021 \text{ kg-m}^2,\ \tau_{L\_rated} = 2.0337 \text{ N-m}, \\ I_{\max} = 2.77 \text{ A},\ V_{\max} = 230 \text{ V}. \end{aligned}$$

Figure 1 shows a block diagram of the speed sensorless control system. The induction motor model for the simulation is based on equations (1), (2), and (3). In the control scheme, the estimated speed is fed back to a current command field-oriented controller [8].

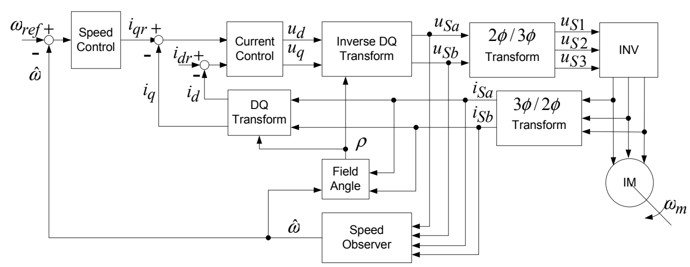

Fig. 1. Sensorless speed observer control system.

Figure 2 shows the simulation results of the motor speed and speed estimator with the motor under full load. From $t = 0$ to $t = 0.4$ seconds, a constant u_{Sa} is applied to the motor to build up the flux and the motor is considered to be held with a brake so that $\omega \equiv 0$. At $t = 0.4$ seconds, the brake is released and the machine is running on a low speed trajectory ($\omega_{\max} = 5\ rad/s$) with full load on the machine from the start. The estimated speed $\hat{\omega}$ is used in the field-oriented controller as shown in Figure 1. In this simulation, the observer gain ℓ in equation (22) was chosen to be 1000.

Figure 3 shows the simulation results of the motor speed and speed estimator with the motor under full load. From $t = 0$ to $t = 0.4$ seconds, a constant u_{Sa} is applied to the motor to build up the flux and the motor is considered to be held with a brake so that $\omega \equiv 0$. At $t = 0.4$ seconds, the brake is released and the machine is controlled to a zero speed trajectory ($\omega \equiv 0$) with full load on the machine. $\hat{\omega}$ is used in the field-oriented controller as shown in Figure 1. The observer gain ℓ in equation (22) was again chosen to be 1000.

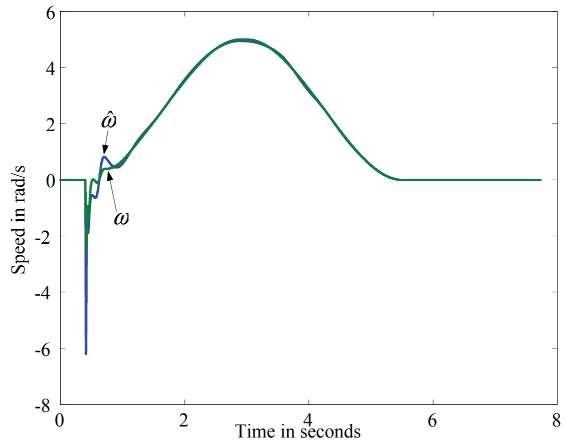

Fig. 2. ω and $\hat{\omega}$ with the motor tracking a low speed trajectory ($\omega_{\max} = 5\ rad/s$) with full load on the machine from the start.

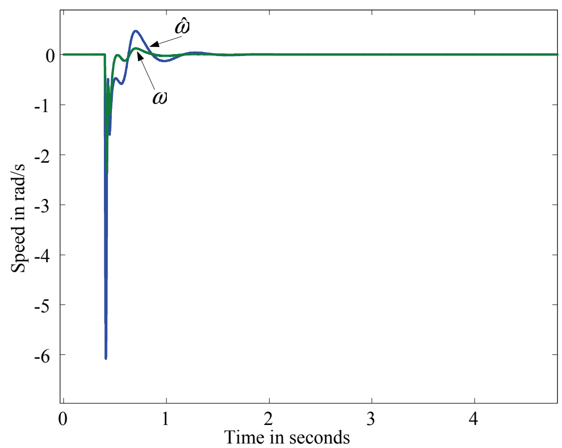

Fig. 3. ω and $\hat{\omega}$ with the motor tracking a zero speed trajectory ($\omega \equiv 0$) with full load on the machine from the start.

VI. Experimental Results

A three-phase 0.5 hp induction motor was used for the experiment. This machine has the same parameters used in the simulations above. A 10 kHz PWM inverter was used to drive the induction motor and a 4096 pulse/rev optical encoder was attached to the motor for position measurements. A 0.5 hp DC motor was coupled to the induction motor as a mechanical load. The real-time computing system RTLAB from Opal RT with a fully integrated hardware and software system was used to provide the control signal [17]. Both a low speed and a zero speed trajectory were run. In both experiments, the motor speed ω was fed back to the field-oriented controller rather than $\hat{\omega}$. The stator voltages and currents were collected and sampled at $120\ \mu s$. A 3rd order Butterworth filter with cutoff frequency of 30 Hz was used to filter the measured stator voltages and currents. The speed observer (22) was used to obtain the estimated speed $\hat{\omega}$. Simulations indicate a significant improvement in tracking if faster sampling rates are possible.

Figure 4 shows the experimental results of the motor speed and speed estimator with the motor under full load. From $t = 0$ to $t = 0.4$ seconds, $u_{Sa} = 10$ V and $u_{Sb} = 0$ is applied to the motor to build up the flux. At $t = 0.4$ seconds, the field-oriented controller was used to control the machine running on a low-speed trajectory ($\omega_{\max} = 5\ rad/s$) with full load.

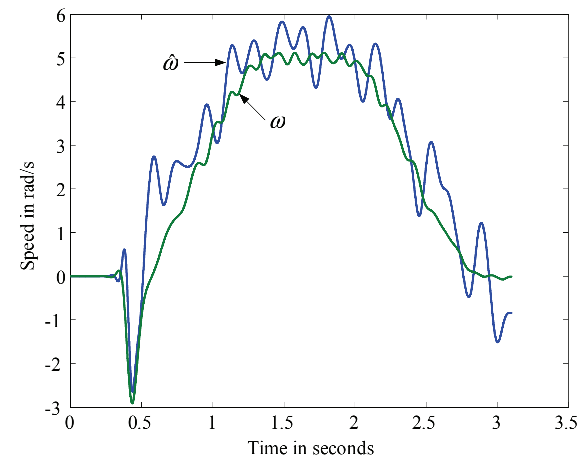

Fig. 4. Motor speed ω and estimated speed $\hat{\omega}$ with the motor tracking a low speed trajectory ($\omega_{\max} = 5\ rad/s$) with full load from the start.

Figure 5 shows the experimental results of the motor speed and speed estimator with the motor under full load.

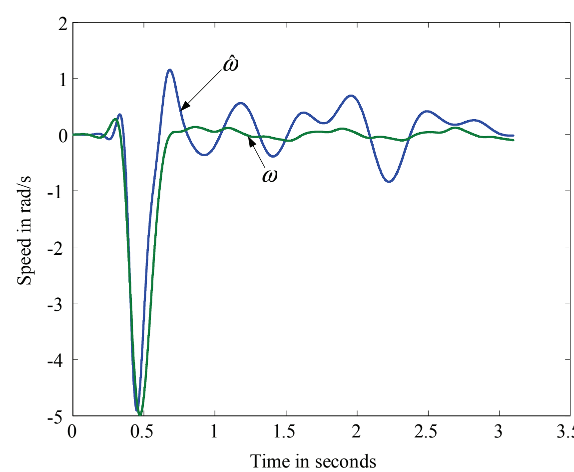

Fig. 5. Motor speed ω and estimated speed $\hat{\omega}$ with the motor tracking a zero speed trajectory ($\omega \equiv 0$) with full load from the start.

From $t = 0$ to $t = 0.4$ seconds, $u_{Sa} = 10$ V and $u_{Sb} = 0$ is applied to the motor to build up the flux. At $t = 0.4$ seconds, the field-oriented control was used to control the machine running at a zero speed trajectory ($\omega \equiv 0$) with full load.

VII. Conclusions

This paper introduced a new approach to speed sensorless control of an induction motor by using an algebraic estimate of the speed to stabilize a dynamic speed observer. This observer is stable, does not require any sort of "slowly varying" speed assumption, and works at zero speed. The singularities of the observer (i.e., when the leading coefficients of the polynomials in ω are zero) were characterized under steady-state conditions. The method used 3rd order derivatives of the currents and 2nd order derivatives of the voltages which in turn requires a fast sample rate to accurately compute them. Experimental results of the speed estimator were presented under open-loop conditions.

VIII. Appendix: Steady-State Expressions

In the following, ω_S denotes the stator frequency and S denotes the normalized slip defined by $S \triangleq (\omega_S - n_p\omega)/\omega_S$. With $u_{Sa} + ju_{Sb} = \underline{U}_S e^{j\omega_S t}$ and $i_{Sa} + ji_{Sb} = \underline{I}_S e^{j\omega_S t}$, it is shown in [8] under steady-state conditions that the complex phasors $\underline{U}_S$ and $\underline{I}_S$ are related by

$$\begin{aligned}\underline{I}_S &= \frac{\underline{U}_S}{R_S + j\omega_S L_S\left(\dfrac{1 + j\frac{S}{S_p}}{1 + j\frac{S}{\sigma S_p}}\right)}\\ &= \frac{\underline{U}_S}{\left(R_S + \frac{(1-\sigma)S\omega_S^2 L_S T_R}{1+S^2\omega_S^2 T_R^2}\right) + j\frac{\omega_S L_S\left(1+\sigma S^2\omega_S^2 T_R^2\right)}{1+S^2\omega_S^2 T_R^2}}\end{aligned}$$

where $S_p \triangleq \frac{R_R}{\sigma\omega_S L_R} = \frac{1}{\sigma\omega_S T_R}$.

A. Steady-state expressions for q_2, q_1, and q_0

The steady-state expressions for q_2, q_1, and q_0 are now derived. These expressions are then used to show that $q_2 > 0$ for $\omega \neq 0$, $q_2 \equiv 0$ for $\omega = 0$, and $q_1 \neq 0$ if $q_2 \equiv 0$. The explicit expression for q_2 is

$$\begin{aligned}q_2 \triangleq n_p^2 \times &\Bigg(\frac{1}{4}\sigma L_S T_R^2\left(\frac{d\left(i_{Sa}^2 + i_{Sb}^2\right)}{dt}\right)^2\\ &- T_R^2\frac{d\left(i_{Sa}^2 + i_{Sb}^2\right)}{dt}\left(u_{Sa}i_{Sa} + u_{Sb}i_{Sb}\right)\\ &+ \frac{T_R^2}{\sigma L_S}\left(i_{Sa}^2 + i_{Sb}^2\right)\left(u_{Sa}^2 + u_{Sb}^2\right)\\ &+ \left(-\frac{\beta M}{T_R} + 2\gamma\right)\frac{1}{4}\sigma L_S T_R^2\frac{d\left(i_{Sa}^2 + i_{Sb}^2\right)^2}{dt}\\ &+ \sigma L_S T_R^2\left(i_{Sb}\frac{di_{Sa}}{dt} - i_{Sa}\frac{di_{Sb}}{dt}\right)^2\\ &+ 2T_R^2\left(i_{Sb}\frac{di_{Sa}}{dt} - i_{Sa}\frac{di_{Sb}}{dt}\right)\left(u_{Sb}i_{Sa} - u_{Sa}i_{Sb}\right)\\ &\left(-\frac{\beta M}{T_R} + \gamma\right)\sigma L_S\gamma T_R^2\left(i_{Sa}^2 + i_{Sb}^2\right)^2\\ &+ \left(\frac{\beta M}{T_R} - 2\gamma\right)T_R^2\left(i_{Sa}^2 + i_{Sb}^2\right)\left(u_{Sa}i_{Sa} + u_{Sb}i_{Sb}\right)\Bigg).\end{aligned}$$

In steady state, let (see [8])

$$\begin{aligned}u_{Sa} + ju_{Sb} &= \underline{U}_S e^{j\omega_S t}\\ i_{Sa} + ji_{Sb} &= \underline{I}_S e^{j\omega_S t}.\end{aligned}$$

The complex phasors $\underline{U}_S$ and $\underline{I}_S$ are related by

$$\underline{I}_S = \frac{\underline{U}_S}{R_S + j\omega_S L_S\left[\frac{1+j\frac{S}{S_p}}{1+j\frac{S}{\sigma S_p}}\right]}.$$

Here $S_p \triangleq \frac{R_R}{\sigma\omega_S L_R} = \frac{1}{\sigma\omega_S T_R}$ so that

$$\begin{aligned}\underline{I}_S &= \frac{\underline{U}_S}{R_S + j\omega_S L_S\left[\frac{1+jS\sigma\omega_S T_R}{1+jS\omega_S T_R}\right]}\\ &= \frac{\underline{U}_S}{\left(R_S + \frac{(1-\sigma)S\omega_S^2 L_S T_R}{1+S^2\omega_S^2 T_R^2}\right) + j\frac{\omega_S L_S\left(1+\sigma S^2\omega_S^2 T_R^2\right)}{1+S^2\omega_S^2 T_R^2}}\end{aligned}$$

Further,

$$u_{Sa}i_{Sa} + u_{Sb}i_{Sb} = \mathrm{Re}\left(\underline{U}_S\underline{I}_S^*\right)$$

$$u_{Sb}i_{Sa} - u_{Sa}i_{Sb} = \mathrm{Im}\left(\underline{U}_S\underline{I}_S^*\right)$$

and

$$\begin{aligned}i_{Sa}^2 + i_{Sb}^2 &= \left|\underline{I}_S\right|^2\\ u_{Sa}^2 + u_{Sb}^2 &= \left|\underline{U}_S\right|^2\end{aligned}$$

As a result, the 1^{st}, 2^{nd}, and 4^{th} terms of q_2 are all zero, i.e.,

$$n_p^2\frac{1}{4}\sigma L_S T_R^2\left(\frac{d\left(i_{Sa}^2 + i_{Sb}^2\right)}{dt}\right)^2 = 0$$

$$-n_p^2 T_R^2\frac{d\left(i_{Sa}^2 + i_{Sb}^2\right)}{dt}\left(u_{Sa}i_{Sa} + u_{Sb}i_{Sb}\right) = 0$$

and

$$n_p^2\left(-\frac{\beta M}{T_R} + 2\gamma\right)\frac{1}{4}\sigma L_S T_R^2\frac{d\left(i_{Sa}^2 + i_{Sb}^2\right)^2}{dt} = 0.$$

The 3^{rd} term of q_2 is given by

$$n_p^2\frac{T_R^2}{\sigma L_S}\left(i_{Sa}^2 + i_{Sb}^2\right)\left(u_{Sa}^2 + u_{Sb}^2\right) = n_p^2\frac{T_R^2}{\sigma L_S}\left|\underline{I}_S\right|^2\left|\underline{U}_S\right|^2.$$

The 5^{th} term of q_2 is given by

$$\begin{aligned}&n_p^2\sigma L_S T_R^2\left(i_{Sb}\frac{di_{Sa}}{dt} - i_{Sa}\frac{di_{Sb}}{dt}\right)^2\\ &= n_p^2\frac{\sigma L_S T_R^2\omega_S^2\left|\underline{I}_S\right|^2\left|\underline{U}_S\right|^2}{\left(R_S + \frac{(1-\sigma)S\omega_S^2 L_S T_R}{1+S^2\omega_S^2 T_R^2}\right)^2 + \frac{\omega_S^2 L_S^2\left(1+\sigma S^2\omega_S^2 T_R^2\right)^2}{\left(1+S^2\omega_S^2 T_R^2\right)^2}}.\end{aligned}$$

The 6^{th} term of q_2 is

$$\begin{aligned}&n_p^2 2T_R^2\left(i_{Sb}\frac{di_{Sa}}{dt} - i_{Sa}\frac{di_{Sb}}{dt}\right)\left(u_{Sb}i_{Sa} - u_{Sa}i_{Sb}\right)\\ &= n_p^2\frac{-2T_R^2\omega_S\left|\underline{I}_S\right|^2\left|\underline{U}_S\right|^2\frac{\omega_S L_S\left(1+\sigma S^2\omega_S^2 T_R^2\right)}{1+S^2\omega_S^2 T_R^2}}{\left(R_S + \frac{(1-\sigma)S\omega_S^2 L_S T_R}{1+S^2\omega_S^2 T_R^2}\right)^2 + \frac{\omega_S^2 L_S^2\left(1+\sigma S^2\omega_S^2 T_R^2\right)^2}{\left(1+S^2\omega_S^2 T_R^2\right)^2}}.\end{aligned}$$

The 7^{th} term of q_2 is

$$\begin{aligned}&n_p^2\left(-\frac{\beta M}{T_R} + \gamma\right)\sigma L_S\gamma T_R^2\left(i_{Sa}^2 + i_{Sb}^2\right)^2\\ &= n_p^2\frac{\left(\frac{R_s^2}{\sigma L_s} + \frac{(1-\sigma)R_s}{\sigma T_R}\right)T_R^2\left|\underline{I}_S\right|^2\left|\underline{U}_S\right|^2}{\left(R_S + \frac{(1-\sigma)S\omega_S^2 L_S T_R}{1+S^2\omega_S^2 T_R^2}\right)^2 + \frac{\omega_S^2 L_S^2\left(1+\sigma S^2\omega_S^2 T_R^2\right)^2}{\left(1+S^2\omega_S^2 T_R^2\right)^2}}.\end{aligned}$$

The 8^{th} term of q_2 is

$$
\begin{aligned}
&n_p^2\left(\frac{\beta M}{T_R}-2\gamma\right)T_R^2\left(i_{Sa}^2+i_{Sb}^2\right)\left(u_{Sa}i_{Sa}+u_{Sb}i_{Sb}\right)\\
=&n_p^2\frac{-\left(\frac{2R_s}{\sigma L_s}+\frac{1-\sigma}{\sigma T_R}\right)T_R^2\left|\underline{I}_S\right|^2\left|\underline{U}_S\right|^2}{\left(R_S+\frac{(1-\sigma)S\omega_S^2L_ST_R}{1+S^2\omega_S^2T_R^2}\right)^2+\frac{\omega_S^2L_S^2\left(1+\sigma S^2\omega_S^2T_R^2\right)^2}{\left(1+S^2\omega_S^2T_R^2\right)^2}}\\
&\times\left(R_S+\frac{(1-\sigma)S\omega_S^2L_ST_R}{1+S^2\omega_S^2T_R^2}\right).
\end{aligned}
$$

Finally, substituting these steady-state expressions into the expression for q_2, one obtains

$$
\begin{aligned}
q_2=&\frac{n_p^2T_R^2\left|\underline{U}_S\right|^4}{\left(\left(R_S+\frac{(1-\sigma)S\omega_S^2L_ST_R}{1+S^2\omega_S^2T_R^2}\right)^2+\frac{\omega_S^2L_S^2\left(1+\sigma S^2\omega_S^2T_R^2\right)^2}{\left(1+S^2\omega_S^2T_R^2\right)^2}\right)^2}\\
&\times\frac{\omega_S^2L_S(1-\sigma)^2(1-S)}{\sigma\left(1+S^2\omega_S^2T_R^2\right)}. \qquad (23)
\end{aligned}
$$

With $\omega\neq 0$, it is seen that $q_2>0$ and $q_2=0$ if and only if $S=1$ (which is equivalent to $\omega=0$).

Similarly, it can be shown that the steady-state expression for q_1 is

$$
\begin{aligned}
q_1=&\frac{n_p\omega_S\left|\underline{U}_S\right|^4}{\left(\left(R_S+\frac{(1-\sigma)S\omega_S^2L_ST_R}{1+S^2\omega_S^2T_R^2}\right)^2+\frac{\omega_S^2L_S^2\left(1+\sigma S^2\omega_S^2T_R^2\right)^2}{\left(1+S^2\omega_S^2T_R^2\right)^2}\right)^2}\\
&\times\frac{L_S(1-\sigma)^2\left(1-\omega_S^2T_R^2(1-S)^2\right)}{\sigma\left(1+S^2\omega_S^2T_R^2\right)}. \qquad (24)
\end{aligned}
$$

If $\omega=0$, then $S=1$ and $q_1\neq 0$.

Finally, the steady-state expression for q_0 is

$$
\begin{aligned}
q_0=&\frac{-\left|\underline{U}_S\right|^4}{\left(\left(R_S+\frac{(1-\sigma)S\omega_S^2L_ST_R}{1+S^2\omega_S^2T_R^2}\right)^2+\frac{\omega_S^2L_S^2\left(1+\sigma S^2\omega_S^2T_R^2\right)^2}{\left(1+S^2\omega_S^2T_R^2\right)^2}\right)^2}\\
&\times\frac{\omega_S^2L_S(1-\sigma)^2(1-S)}{\sigma\left(1+S^2\omega_S^2T_R^2\right)}. \qquad (25)
\end{aligned}
$$

B. Steady-state expressions for a_2, a_1, and a_0

The steady-state expressions for a_2, a_1, a_0 are

$$
\begin{aligned}
a_2=&\frac{-n_p^2\left|\underline{U}_S\right|^4}{\left(\left(R_S+\frac{(1-\sigma)S\omega_S^2L_ST_R}{1+S^2\omega_S^2T_R^2}\right)^2+\frac{\omega_S^2L_S^2\left(1+\sigma S^2\omega_S^2T_R^2\right)^2}{\left(1+S^2\omega_S^2T_R^2\right)^2}\right)^2}\\
&\times\frac{\omega_S(1-\sigma)^2}{\sigma^2\left(1+S^2\omega_S^2T_R^2\right)}\times\frac{1}{den} \qquad (26)
\end{aligned}
$$

$$
\begin{aligned}
a_1=&\frac{n_p\left|\underline{U}_S\right|^4}{\left(\left(R_S+\frac{(1-\sigma)S\omega_S^2L_ST_R}{1+S^2\omega_S^2T_R^2}\right)^2+\frac{\omega_S^2L_S^2\left(1+\sigma S^2\omega_S^2T_R^2\right)^2}{\left(1+S^2\omega_S^2T_R^2\right)^2}\right)^2}\\
&\times\frac{2\omega_S^2(1-\sigma)^2(1-S)}{\sigma^2\left(1+S^2\omega_S^2T_R^2\right)}\times\frac{1}{den} \qquad (27)
\end{aligned}
$$

and

$$
\begin{aligned}
a_0=&\frac{-\left|\underline{U}_S\right|^4}{\left(\left(R_S+\frac{(1-\sigma)S\omega_S^2L_ST_R}{1+S^2\omega_S^2T_R^2}\right)^2+\frac{\omega_S^2L_S^2\left(1+\sigma S^2\omega_S^2T_R^2\right)^2}{\left(1+S^2\omega_S^2T_R^2\right)^2}\right)^2}\\
&\times\frac{\omega_S^3(1-\sigma)^2(1-S)^2}{\sigma^2\left(1+S^2\omega_S^2T_R^2\right)}\times\frac{1}{den}. \qquad (28)
\end{aligned}
$$

where

$$
\begin{aligned}
den=&n_pT_R\left|\underline{U}_S\right|^4\\
&\times\frac{\left(\frac{(1-\sigma)}{\sigma T_R}\frac{1+S^2\omega_S^2T_R^2-S\omega_S^2T_R^2}{1+S^2\omega_S^2T_R^2}\right)^2+\left(\frac{(1-\sigma)}{\sigma}\frac{\omega_S}{1+S^2\omega_S^2T_R^2}\right)^2}{\left(\left(R_S+\frac{(1-\sigma)S\omega_S^2L_ST_R}{1+S^2\omega_S^2T_R^2}\right)^2+\frac{\omega_S^2L_S^2\left(1+\sigma S^2\omega_S^2T_R^2\right)^2}{\left(1+S^2\omega_S^2T_R^2\right)^2}\right)^2}
\end{aligned}
$$

REFERENCES

[1] K. Rajashekara, A. Kawamura, and K. Matsuse, eds., *Sensorless Control of AC Motor Drives - Speed and Position Sensorless Operation*. IEEE Press, 1996.

[2] P. Vas, *Sensorless Vector Control and Direct Torque Control*. Oxford University Press, 1998.

[3] M. Vélez-Reyes, K. Minami, and G. Verghese, “Recursive speed and parameter estimation for induction machines,” in *Proceedings of the IEEE Industry Applications Conference*, pp. 607–611, 1989. San Diego, California.

[4] M. Vélez-Reyes, W. L. Fung, and J. E. Ramos-Torres, “Developing robust algorithms for speed and parameter estimation in induction machines,” in *Proceedings of the IEEE Conference on Decision and Control*, pp. 2223–2228, 2001. Orlando, Florida.

[5] M. Vélez-Reyes, *Decomposed algorithms for parameter estimation*. PhD thesis, Massachusetts Institute of Technology, 1992.

[6] M. Vélez-Reyes and G. Verghese, “Decomposed algorithms for speed and parameter estimation in induction machines,” in *Proceedings of the IFAC Nonlinear Control Systems Design Symposium*, pp. 156–161, 1992. Bordeaux, France.

[7] M. Bodson and J. Chiasson, “A comparison of sensorless speed estimation methods for induction motor control,” in *Proceedings of the 2002 American Control Conference*, pp. 3076–3081, May 2002. Anchorage, AK.

[8] W. Leonhard, *Control of Electrical Drives*. 3rd Edition, Springer-Verlag, Berlin, 2001.

[9] D. Nešić, I. M. Y. Mareels, S. T. Glad, and M. Jirstrand, “Software for control system analysis and design: symbol manipulation,” in *Encyclopedia of Electrical Engineering*, John Wiley & Sons, J. Webster, Editor, 2001. available online at http://www.interscience.wiley.com:83/eeee/.

[10] M. Diop and M. Fliess, “On nonlinear observability,” in *Proceedings of the 1st European Control Conference*, pp. 152–157, Hermès, Paris, 1991.

[11] M. Diop and M. Fliess, “Nonlinear observability, identifiability and persistent trajectories,” in *Proceedings of the 36th Conference on Decision and Control*, pp. 714–719, Brighton England, 1991.

[12] M. Fliess and H. Síra-Ramirez, “Control via state estimation of some nonlinear systems,” in *Symposium on Nonlinear Control Systems (NOLCOS-2004)*, September 2004. Stuttgart, Germany.

[13] S. Ibarra-Rojas, J. Moreno, and G. Espinosa-Pérez, “Global observability analysis of sensorless induction motors,” *Automatica*, vol. 40, pp. 1079–1085, 2004.

[14] M. Li, J. Chiasson, M. Bodson, and L. M. Tolbert, “Observability of speed in an induction motor from stator currents and voltages,” in *IEEE Conference on Decision and Control*, pp. 3438–3443, December 2005. Seville Spain.

[15] J. Chiasson, *Modeling and High-Performance Control of Electric Machines*. John Wiley & Sons, 2005.

[16] W. J. Rugh, *Linear System Theory*. 2nd Edition, Prentice-Hall, 1996.

[17] Opal-RT Technologies, “RT-LAB,” See http://www.opal-rt.com.